Available online at www.sciencedirect.com
ScienceDirect
Dyes and Pigments 75 (2007) 507–515
DYES and PIGMENTS
www.elsevier.com/locate/dyepig

Synthesis, crystal structures and spectral characterization of *trans*-bisaquabis(*o*-vanillinato)copper(II), *cis*-aquabis (*o*-vanillinato)copper(II) and aqua[bis(*o*-vanillinato)-1, 2-ethylenediimin]copper(II)

Mustafa Odabaşoğlu [a,*], Figen Arslan [a], Halis Ölmez [a], Orhan Büyükgüngör [b]

[a] *Faculty of Arts and Sciences, Department of Chemistry, Ondokuz Mayis University, TR-55139 Kurupelit, Samsun, Turkey*
[b] *Department of Physics, Ondokuz Mayis University, TR-55139 Kurupelit, Samsun, Turkey*

Received 24 November 2005; received in revised form 6 March 2006; accepted 22 June 2006
Available online 8 September 2006

Abstract

trans-Bisaquabis(*o*-vanillinato)copper(II) (**I**), *cis*-aquabis(*o*-vanillinato)copper(II) (**II**) and aqua[bis(*o*-vanillinato)-1,2-ethylenediimin]copper(II) (**III**) complexes were synthesized and characterized by means of elemental analysis, IR and UV–vis spectroscopy, thermal analysis and X-ray diffraction techniques. The coordination geometry around Cu(II) is a octahedral with coordination number of six for **I** and is a square-pyramidal with coordination number of five for both **II** and **III**. In all three compounds, a three-dimensional structure is formed via C–H···O hydrogen-bond interactions and intermolecular π–π and π-ring interactions. The compounds **I** and **III** have two-dimensional hydrogen-bonded step-chain structure in *xz*-plane, while compound **II** has a zigzag chain structure in *xy*-plane. On the basis of the first DTA_{max} of the anhydrous complexes of **I** and **II**, the thermal stability sequence is *trans*-isomer > *cis*-isomer. This fact should be related with the binding of the ligand.

Keywords: Schiff base complexes; *o*-Vanillinato ligand; Copper complexes; Thermal decomposition; Crystal structure

1. Introduction

The investigation of Schiff base complexes has been of interest for many years to help understanding the interactions between metal ions and proteins or as other biological references. Recent years have witnessed a great deal of interest in the synthesis and characterization of transition metal complexes containing Schiff bases as ligands due to their application as catalysts for many reactions [1–3] and relation to synthetic and natural oxygen carriers [4] and also use as new structural probes in nucleic acids' chemistry and as therapeutic agents [5–8]. Furthermore, Schiff bases are facing with growing interest and they may have numerous applications, e.g. as anticancer [9,10], antibacterial [11], antiviral [12], antifungal [13], and about their other biological properties [14,15]. They also contain N=C···C=N structural unit, which forms a strong chelate ring giving possible electron delocalization associated with extended conjugation that may affect the nature of the complex formed. Particularly the first rows of transition metal complexes with such ligands have a wide range of biological properties [16–18]. Our current interest is to prepare a series of *o*-vanillinato and their Schiff base-Cu(II) chelated model compounds and the investigation of their molecular and crystal structures by IR and UV–vis spectroscopy, thermal analysis and X-ray technique. The present study reports the new products (**I** and **II**) and a product (**III**) investigated in Cambridge Database before but presented in wrong space group and with no coordinates [19]. The

* Corresponding author. Tel.: +90 362 4576020; fax: +90 362 4576081.
E-mail address: muodabas@omu.edu.tr (M. Odabaşoğlu).

0143-7208/$ - see front matter © 2006 Elsevier Ltd. All rights reserved.
doi:10.1016/j.dyepig.2006.06.033

trans-aquabis(*o*-vanillinato)Cu(II) (**I**) was obtained by the reaction of *o*-vanillin and $Cu(CH_3COO)_2 \cdot 2H_2O$, the *cis*-aquabis(*o*-vanillinato)Cu(II) (**II**) was obtained by the reaction of 2-(3-methoxysaliciylidene amino)-1*H*-benzimidazole [20] and $Cu(CH_3COO)_2 \cdot 2H_2O$ and then aqua[bis(*o*-vanillinato)-1,2-ethylenediimin]Cu(II) (**III**) was prepared by the reaction of **II** with 1,2-ethylenediamine (Scheme 1).

2. Experimental

2.1. Synthesis

Copper acetate dihydrate, $Cu(CH_3COO)_2 \cdot 2H_2O$, (1.00 mmol, 0.19 g) was dissolved in ethanol (75 ml) and then *o*-vanillin (2.00 mmol, 0.30 g) dissolved in ethanol was added to this solution. The mixture was refluxed for 1 h, allowed to cool and the solvent was removed. The resulting green powder was recrystallized in ethanol–methanol mixture (1:2). Yield for **I**: 90%; m.p. 522–524 K. Elemental analysis found (calculated for $C_{16}H_{18}O_8Cu$, **I**): C, 47.35 (47.82); H, 4.78 (4.51).

Copper acetate dihydrate, $Cu(CH_3COO)_2 \cdot 2H_2O$, (1.00 mmol, 0.19 g) was dissolved in ethanol and then 2-(3-methoxysaliciylidene amino)-1*H*-benzimidazole (2.00 mmol, 0.57 g) dissolved in ethanol was added to this solution. The mixture was refluxed for 2 h, allowed to cool and the solvent was removed. The resulting green powder was recrystallized in methanol. Yield for **II**: 74%; m.p. 506–508 K. Elemental analysis found (calculated for $C_{16}H_{16}O_7Cu$, **II**): C, 49.89 (50.07); H, 4.53 (4.20).

The previously obtained **II** (1.00 mmol, 0.38 g) was dissolved in methanol (100 ml) and added dropwise with stirring at 323 K to ethylenediamine (1.00 mmol, 0.06 g) which also was dissolved in methanol (25 ml). The reaction mixture was then cooled to room temperature. The green crystals formed were filtered and washed with 10 ml of acetone. Yield for **III**: 81%; m.p. 530–533 K. Elemental analysis found (calculated for $C_{18}H_{20}N_2O_5Cu$, **III**): C, 53.21 (53.00); H, 4.56 (4.94); N, 6.82 (6.87).

2.2. Physical measurements

Elemental analyses were performed by standard methods at TUBITAK (The Scientific and Technological Research Council of Turkey). The UV–vis spectra were obtained for the methanol solution of the complexes with a Unicam UV2 spectrometer in the range 900–200 nm. The IR spectra were recorded on a Jasco 430 FT/IR spectrophotometer using KBr pellets and operating at 4000–200 cm^{-1}. TG8110 thermal analyzer was used to record simultaneous TG and DTA curves in static air atmosphere at a heating rate of 10 K min^{-1} in the temperature range of 20–700 °C using platinum crucibles. Highly sintered α-Al_2O_3 was used as a reference and the DTG sensitivity was 0.05 mg s^{-1}.

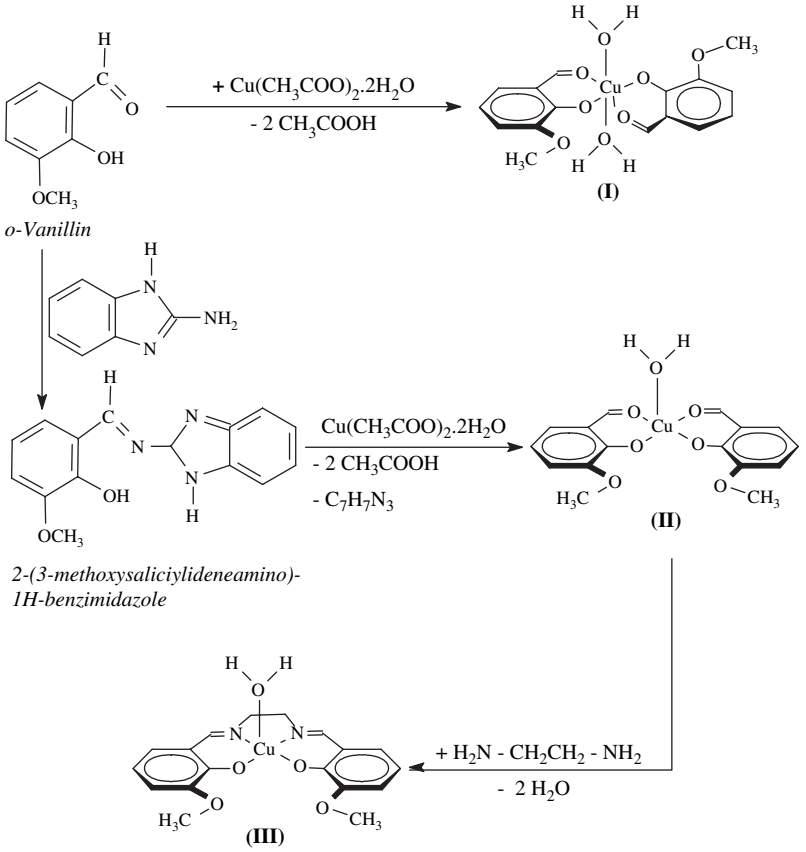

Scheme 1.

Table 1
Summarized crystallographic data for complexes of **I**, **II** and **III**

Formula	$C_{16}H_{18}O_8Cu$ (**I**)	$C_{16}H_{16}O_7Cu$ (**II**)	$C_{18}H_{20}N_2O_5Cu$ (**III**)
Molecular weight	401.84	383.83	407.9
Temperature	296(2) K	100(2) K	100(2) K
Wavelength	0.71073 Å	0.71073 Å	0.71073
Crystal system	Monoclinic	Orthorhombic	Orthorhombic
Space group	*P*21/*c*	Pb_{ca}	*Pnma*
Unit cell dimensions	$a = 6.7635(5)$	$a = 11.6481(7)$	$a = 9.2590(12)$
	$b = 23.485(2)$	$b = 18.0349(10)$	$b = 24.701(3)$
	$c = 5.1553(4)$	$c = 14.9867(11)$	$c = 7.5180(10)$
	$\alpha = 90.00°$	$\alpha = 90$	$\alpha = 90$
	$\beta = 97.304(6)°$	$\beta = 90$	$\beta = 90$
	$\gamma = 90.00°$	$\gamma = 90$	$\gamma = 90$
Volume	812.21(12) $Å^3$	3148.3(3) $Å^3$	1719.4(4) $Å^3$
Z	2	8	4
Calculated density	1.627 Mg m^{-3}	1.620 Mg m^{-3}	1.576 Mg m^{-3}
μ	1.39 mm^{-1}	1.42 mm^{-1}	1.303 mm^{-1}
F(000)	414	1576	844
Crystal size (mm)	0.46 × 0.20 × 0.06	0.33 × 0.25 × 0.11	0.22 × 0.15 × 0.01
θ range	1.73–26.05	2.26–27.95	2.20–25.57
Index ranges	$-7 \le h \le 8$	$-14 \le h \le 14$	$-11 \le h \le 11$
	$-28 \le k \le 28$	$-19 \le k \le 22$	$-29 \le k \le 29$
	$-6 \le l \le 6$	$-18 \le l \le 16$	$-9 \le l \le 8$
Independent reflections	1595	3104	1643
Reflections observed ($>2\sigma$)	1289	2233	1036
Goodness-of-fit on F^2	1.038	0.921	0.827
R, R_w [$I > 2\sigma(I)$]	0.384, 0.0993	0.0381, 0.0848	0.384, 0.0966
R_{int} indices (all data)	0.1055	0.0763	0.0852

2.3. Crystal structure analysis

For **I** and **III**, except the freely refined H atoms bounded to aqua O atom, all H atoms were refined using riding model for hydrogen bonds with d(C–H) = 0.93–0.96–0.97 Å. The U_{iso} values for these H atoms were assigned to 1.2 U_{eq}(C) [1.5 U_{eq}(methyl C)]. For **II**, all H atoms were refined freely with C–H = 0.81(3)–1.05(3) Å, and U_{iso}(H) = 0.032(9)–0.070(13) $Å^2$ except the hydrogens of aqua O atom with fixed O–H = 0.83(2) Å. A summary of crystallographic data, experimental details, and refinement results for compounds **I**, **II** and **III** are given in Table 1.

For all compounds, data collection: Stoe X-AREA [21]; cell refinement: Stoe X-AREA [21]; data reduction: Stoe X-RED32 [21]; program(s) used to solve structures: SHELXS97 [22]; program(s) used to refine structures: SHELXL97 [22];

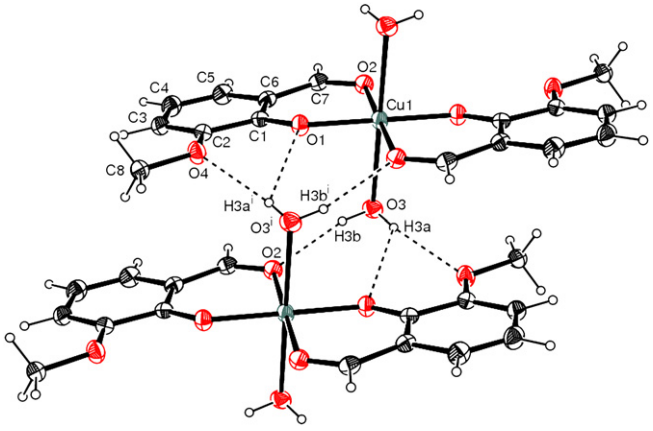

Fig. 1. An ORTEP [23] dimeric view of **I**, with the atom-numbering scheme and 30% probability displacement ellipsoids.

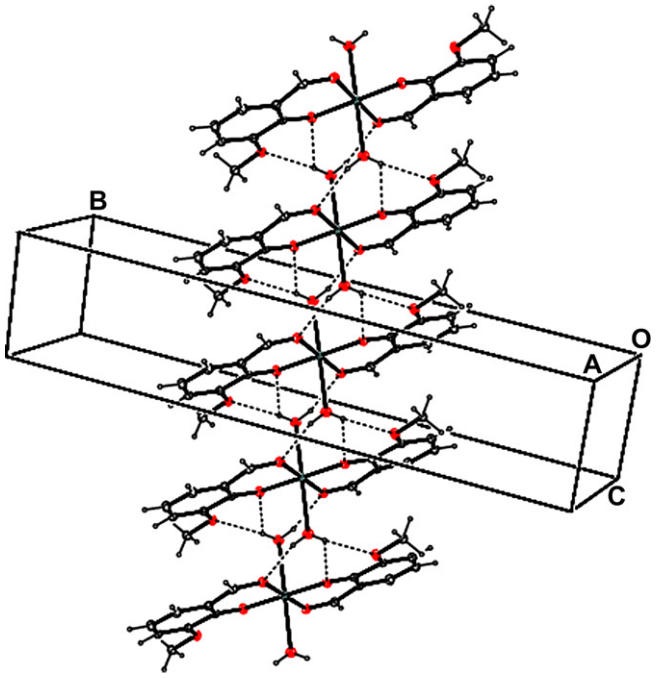

Fig. 2. An ORTEP [23] view of the hydrogen-bonded step-chain diagram of **I**.

Table 2
Selected geometric parameters (Å, °) for **I**

C1–O1	1.289(3)	C1–C6	1.413(4)
C6–C7	1.428(4)	C7–O2	1.249(4)
O1–Cu1	1.9174(19)	O2–Cu1	1.989(2)
O3–Cu1	2.428(2)		
C1–C6–C7	122.2(3)	O1–C1–C6	125.5(2)
C1–O1–Cu1	126.34(18)	O2–C7–C6	127.1(3)
O1–Cu1–O1i	180.00(6)	C7–O2–Cu1	124.55(19)
O2–Cu1–O3	88.96(9)	O1–Cu1–O2	92.27(8)
O1–Cu1–O3	88.71(9)		
C6–C7–O2–Cu1	5.0(4)	C4–C5–C6–C7	−175.3(3)

Symmetry codes: (i) $1-x$, $1-y$, $1-z$.

Table 3
Hydrogen-bonding geometry (Å, °) for **I**

D–H···A	D–H	H···A	D···A	D–H···A
O3–H3A···O4i	0.74(5)	2.19(5)	2.929(4)	172(5)
O3–H3A···O1i	0.74(5)	2.55(5)	3.014(3)	122(4)
O3–H3B···O2ii	0.81(5)	2.08(5)	2.881(3)	167(5)
C7–H7···O3iii	0.93	2.40	3.319(4)	168.3

Symmetry codes: (i) $1-x$, $1-y$, $-z$; (ii) x, y, $z-1$; (iii) $-x$, $1-y$, $1-z$.

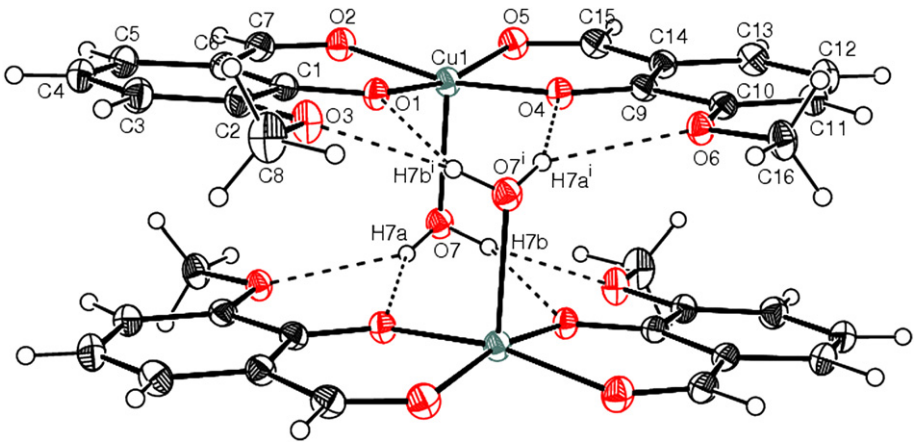

Fig. 3. An ORTEP [23] dimeric view of **II**, with the atom-numbering scheme and 30% probability displacement ellipsoids.

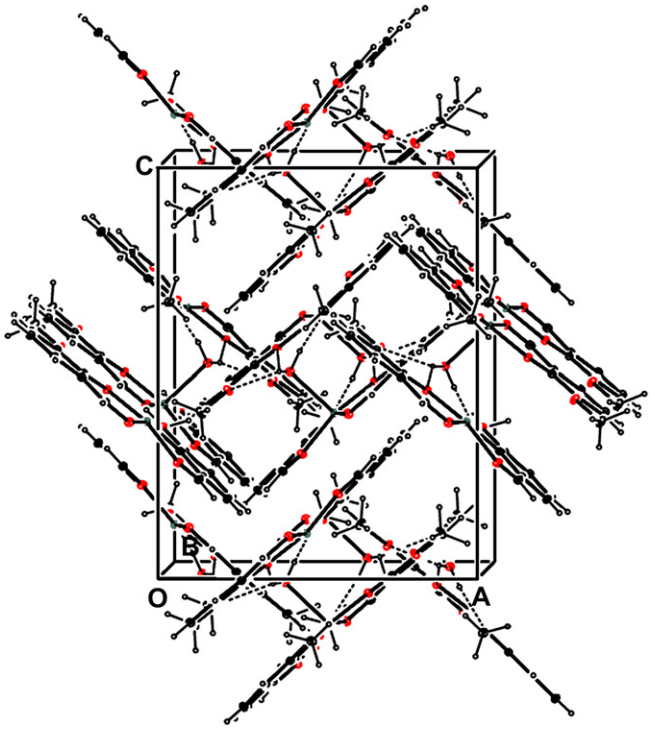

Fig. 4. An ORTEP [23] view of the packing diagram of **II**.

molecular graphics: ORTEP3 for Windows [23]; software used to prepare material for publication: WinGX [24].

3. Results and discussion

3.1. Description of the crystal structure

The dimeric molecular structure and two-dimensional hydrogen-bonded step-chain diagrams of **I** are illustrated in Figs. 1 and 2, respectively, and selected bond distances and angles are listed in Table 2. The molecule of **I** possesses inversion center on Cu1 atom surrounded by two *trans-o*-vanillinato ligands and two water molecules forming an octahedral

Table 4
Selected geometric parameters (Å, °) for **II**

C1–O1	1.299(3)	C1–C6	1.417(4)
C6–C7	1.404(4)	C7–O2	1.257(4)
C9–O4	1.299(3)	C9–C14	1.421(4)
C14–C15	1.411(4)	C15–O5	1.256(4)
O1–Cu1	1.9237(18)	O2–Cu1	1.956(2)
O4–Cu1	1.9233(19)	O5–Cu1	1.962(2)
O7–Cu1	2.234 (2)		
O2–C7–C6	127.80(3)	O1–C1–C6	124.7(3)
C1–O1–Cu1	127.69(18)	O5–C15–C14	128.2(3)
C9–O4–Cu1	127.13(18)	C7–O2–Cu1	125.6(2)
O4–Cu1–O2	168.09(8)	C15–O5–Cu1	124.60(19)
O1–Cu1–O5	167.78(8)	O1–Cu1–O2	91.59(8)
O4–Cu1–O7	98.60(8)	O2–Cu1–O5	85.66(9)
O1–Cu1–O7	100.16(8)		
C4–C5–C6–C7	−176.4(3)	C12–C13–C14–C15	178.6(3)
C6–C7–O2–Cu1	8.6(4)	C14–C15–O5–Cu1	−4.7(4)

Table 5
Hydrogen–bonding geometry (Å, °) for **II**

D–H···A	D–H	H···A	D···A	D–H···A
O7–H7A··· O4i	0.829(18)	2.14(3)	2.894(3)	150(3)
O7–H7A··· O6i	0.829(18)	2.22(3)	2.871(3)	136(3)
O7–H7B··· O1i	0.835(18)	2.18(3)	2.914(3)	147(3)
O7–H7B··· O3i	0.835(18)	2.19(3)	2.885(3)	140(3)
C5–H5·····O7ii	1.01(3)	2.55(3)	3.479(4)	153(2)
C4–H4·····O2ii	0.91(4)	2.51(4)	3.254(4)	140(3)
C16–H16C···O5iii	0.94(3)	2.72(4)	3.491(4)	140(3)
C12–H12···O6iv	0.89(3)	2.73(3)	3.470(3)	141(3)
C13–H13···O1iv	0.81(3)	2.51(3)	3.302(4)	167(3)

Symmetry codes: (i) $1-x$, $1-y$, $1-z$; (ii) $x-12$, $32-y$, $1-z$; (iii) $1-x$, $y-12$, $32-z$; (iv) $12+x$, y, $32-z$.

structure with coordination number of six (Fig. 1). The phenolic oxygen atoms lose their protons and gets coordinated to copper. Cu1/O1/O2/C1/C6/C7 atoms define a plane with maximum deviation −0.099(2) Å with O3 atom located in perpendicular position to this plane [Cu1–O3, 2.428(2) Å]. The bond lengths of Cu–O in the basal plane are 1.918(2) Å and 1.989(2) Å and the Cu–O3 bond length [2.428(2) Å] is significantly longer than these Cu–O bonds (Table 2). Similar O–Cu–O bond angles are reported in a previous work of tetragonal pyramidal-Cu complex [25].

The C1/C2/C3/C4/C5/C6 ring (A ring) is involved in an intermolecular C–H···π interaction with C8 [x, y, $-1+z$; 3.639(4) Å; 154.16°]. In addition to this π···ring interactions, there are two five-membered rings and two six-membered rings in the dimeric structure (Fig. 1), formed as a result of the O3···O1, O3···O4 and O3···O2 hydrogen bonds (Table 3).

The dimeric molecular structure and packing diagrams of **II** are illustrated in Figs. 3 and 4, respectively, and selected bond distances and angles are listed in Table 4. The central copper atom is surrounded by two *cis-o*-vanillinato ligands and one water molecule forming a square-pyramidal structure with coordination number of five for Cu. The phenolic oxygen atoms lose their protons and gets coordinated to copper as in **I**. O1/O2/O3/O4 atoms define a plane with maximum deviation 0.0024(2) Å for O2 atom. In **II**, the bond lengths of Cu–O in the basal plane are in the range of 1.923(2)–1.962(2) Å

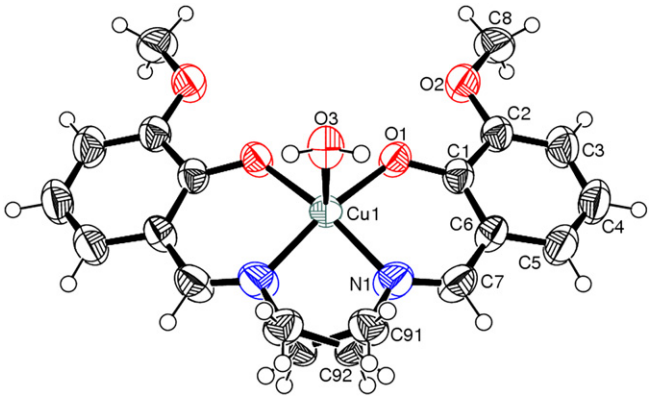

Fig. 5. An ORTEP [23] view of **III**, with the atom-numbering scheme and 50% probability displacement ellipsoids.

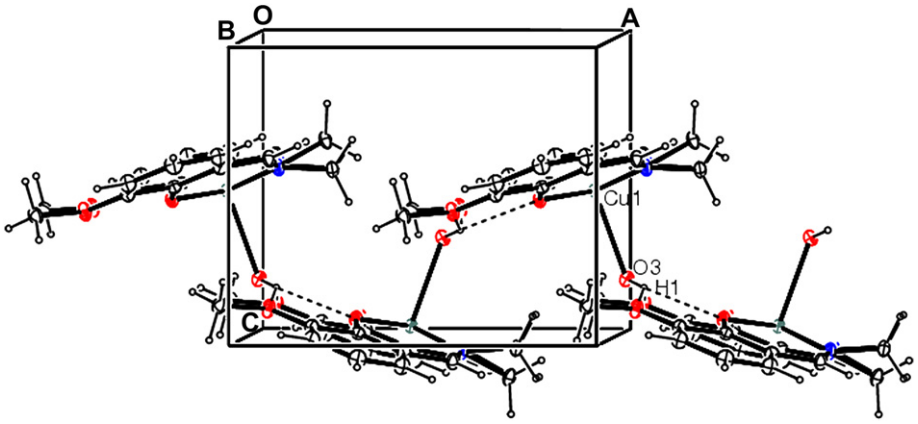

Fig. 6. An ORTEP [23] view of the hydrogen-bonded zigzag chain diagram of **III**.

and the Cu–O7 bond length [2.234(2) Å] is significantly longer than these Cu–O bonds (Table 2). The diagonal O–Cu–O angles are 167.78(8)° and 168.09(8)° and the other O–Cu–O bond angles are in the range of 85.66(9)°–92.65(8)° (Table 2). Similar O–Cu–O bond angles are reported in a previous work of tetragonal pyramidal-Cu complex [25].

In the extended structure of **II**, there are weak intermolecular π–π, π-ring and C–H···O interactions (Table 5). An intermolecular π–π interaction occurs between the phenyl rings (A ring = C1/C2/C3/C4/C5/C6 and B ring = C9/C10/C11/C12/C13/C14) of the neighboring molecules. Ring A is oriented in such a way that the perpendicular distance from A to B is 3.650(2) Å and the closest distance being 3.391(4) Å for C1···C10^{i} [symmetry code: (i) $-x$, $-y$, $1-z$]. Rings A and B are also involved in an intermolecular C–H···π interaction with C3 and C8 atoms of the other aromatic rings; C3–H3···B ring [$1/2-x$, $-y$, $-1/2+z$] 2.83(3) Å [C3···B = 3.687(3) Å], 152(3)° and C8–H8B···D ring (D ring = Cu1/O4/O5/C9/C14/C15) 2.85(4) Å [C8···D = 3.540(4) Å], 128(3)°. In addition to these π–π, π-ring interactions, there are five- and six-membered rings in the dimeric structure (Fig. 2), formed as a result of the O1···H7B, O5···H7B and O3···H7A, O6···H7A hydrogen bonds (Table 5). This set of hydrogen bonding and π–π, π-ring interactions employ most of the available topological features to stabilize the crystal structure.

The molecular structure and two-dimensional hydrogen-bonded zigzag chain diagrams of **III** are illustrated in Figs. 5 and 6, respectively, and selected bond distances and angles are listed in Table 6. The central Cu1 atom in the compound is five-coordinated by two O atoms and two N atoms from the Schiff base ligand and one O atom from the water molecule. The Cu atom is located 0.0015(3) Å out of the basal plane defined by the four donor (O1 and N1) atoms in the complex. As in **I**, the coordination geometry around copper can be described as a near square-pyramidal. The Cu1–O1 bond of 1.927(2) Å is similar to the corresponding value [Cu–O = 1.923(2)–1.962(2) Å] in **II** but Cu–O3 bond length is 2.361(4) Å longer than the equivalence Cu–O7 bond [2.290(2) Å] in **II**, showing an elongation of Cu–O bond. This result may be attributed to the steric hindrance of ethylene bridge.

The value of the two *trans* angles in the basal square-plane of Cu1 is symmetry equivalent with the value of [167.38(12)°] indicating a slightly distorted square planar geometry of Cu1. There is an overall ‘‘butterfly‘‘ shape to the molecule, as evidenced by a dihedral angle of 52.7(5)° between the two *o*-vanillylidene ring systems of the complex. The dihedral angle between the CuN2O2 square-plane and the *o*-vanillylidene ring system is 28.6(3)°. The two C atoms connecting 1,2-diaminethane show positional disorder with occupancy factors of 0.48(3) and 0.52(3).

This type of disorder is quite common and is observed, for example, in some transition metal complexes with Schiff base ligands [26,27]. As in **II**, there are also weak intermolecular

Table 6
Selected geometric parameters (Å, °) for **III**

C1–O1	1.315(4)	C1–C6	1.417(5)
C6–C7	1.425(5)	C7–N1	1.276(5)
C91–N1	1.449(10)	C92–N1	1.559(12)
N1–Cu1	1.947(3)	O1–Cu1	1.928(2)
O3–Cu1	2.362(4)		
C1–C6–C7	122.9(3)	O1–C1–C6	124.8(3)
C7–N1–C91	117.9(5)	N1–C7–C6	125.2(3)
C7–N1–Cu1	127.7(3)	C7–N1–C92	120.8(4)
C92–N1–Cu1	108.4(5)	C91–N1–Cu1	113.2(5)
O1–Cu1–N1	91.98(12)	C1–O1–Cu1	127.1(2)
N1–Cu1–O3	93.87(13)	O1–Cu1–O3	97.90(10)
C6–C7–N1–Cu1	2.7(6)	C4–C5–C6–C7	−179.0(4)

Table 7
Hydrogen-bonding geometry (Å, °) for **III**

D–H···A	D–H	H···A	D···A	D–H···A
O3–H1···O1i	0.81(3)	2.29(3)	3.005(4)	146(4)
O3–H1···O2i	0.81(3)	2.23(4)	2.923(3)	143(3)
C8–H8A···O1ii	0.96	2.86	3.639(5)	139.3

Symmetry codes: (i) $12+x$, y, $32-z$; (ii) $x-12$, y, $32-z$.

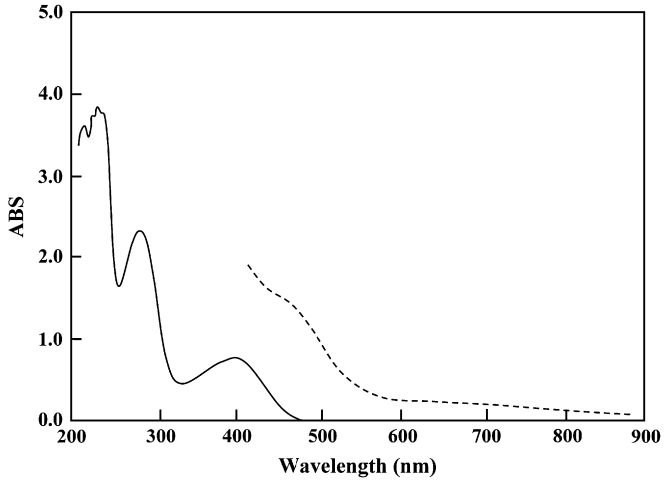

Fig. 7. UV–vis spectra of compounds **I** in methanol, 1.3×10^{-4} M (—) and 1.3×10^{-3} M (- - - -).

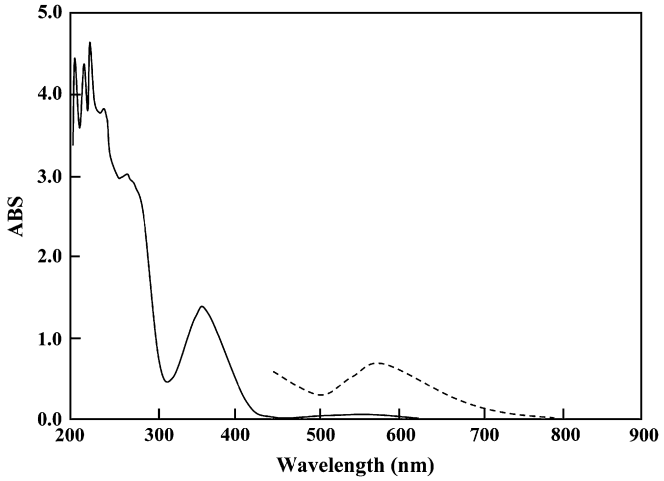

Fig. 9. UV–vis spectra of compounds **III** in methanol, 1.9×10^{-4} M (—) and 1.9×10^{-3} M (- - - -).

π–π, π-ring and C–H···O and O–H···O hydrogen-bond interactions in **III** (Table 7).

3.2. Spectra characteristics

The electronic spectra are measured at room temperature in methanol for the title complexes in the range of 200–900 nm. The electronic spectrum of **I** (Fig. 7) exhibits a very broad d–d absorption transition centered at 631 nm ($\varepsilon = 283\ \mathrm{L\,mol^{-1}\,cm^{-1}}$). This band is assigned to the $^2E_g \rightarrow {}^2T_{2g}$ d–d transition. The d–d transition spectrum of **II** (Fig. 8) is compatible with distorted square-pyramidal configuration. The maximal absorption is at 678 nm and ε value is $75\ \mathrm{L\,mol^{-1}\,cm^{-1}}$. This band is assigned to the $a_1 \rightarrow b_1$ d–d transition. The charge transfer bands for **I** and **II** appear at 396 nm ($\varepsilon = 6038\ \mathrm{L\,mol^{-1}\,cm^{-1}}$) and 395 nm ($\varepsilon = 6276\ \mathrm{L\,mol^{-1}\,cm^{-1}}$), respectively.

The electronic spectrum of **III** exhibits three absorption bands (Fig. 9). The bands at 274 nm ($\varepsilon = 16\,722\ \mathrm{L\,mol^{-1}\,cm^{-1}}$) and 368 nm ($\varepsilon = 7833\ \mathrm{L\,mol^{-1}\,cm^{-1}}$) have been assigned to $\pi \rightarrow \pi^*$ and $n \rightarrow \pi^*$ transitions of *o*-vanillinato-1,2-ethylenediimin ligand, respectively. Third band observed at 572 nm ($\varepsilon = 266\ \mathrm{L\,mol^{-1}\,cm^{-1}}$) is assigned to the $a_1 \rightarrow b_1$ d–d transition.

The IR spectra of **I** and **II** display a strong absorption band at 1610 $\mathrm{cm^{-1}}$ and 1608 $\mathrm{cm^{-1}}$, respectively, which are assigned to ν (C=O) stretching mode in *o*-vanillinato ligands. The stretching band of **III** observed at 1641 $\mathrm{cm^{-1}}$ is assigned to

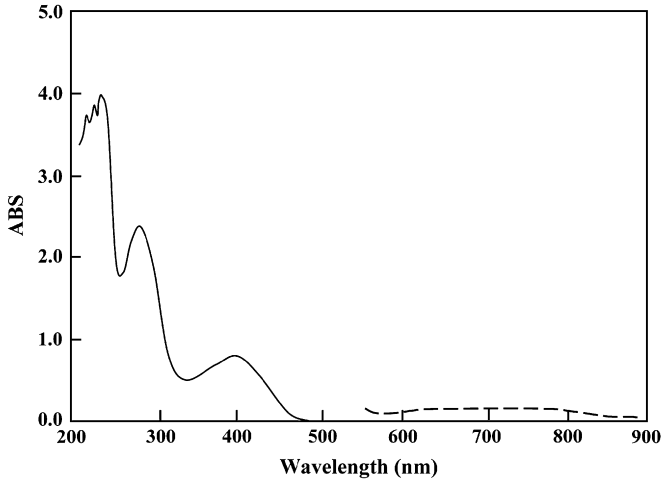

Fig. 8. UV–vis spectra of compounds **II** in methanol, 1.3×10^{-4} M (—) and 1.3×10^{-3} M (- - - -).

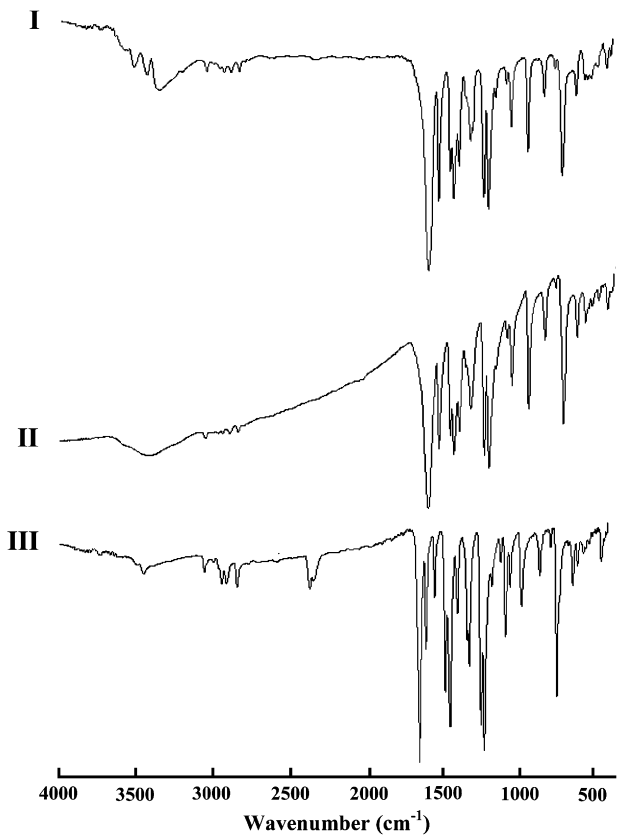

Fig. 10. FT-IR spectra of compounds **I**, **II** and **III** in the solid state (KBr).

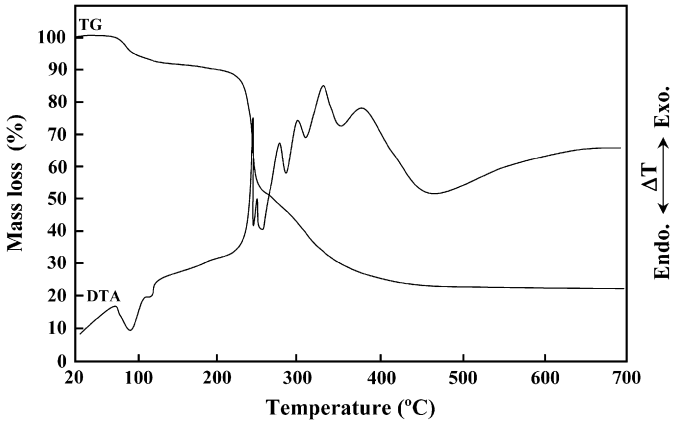

Fig. 11. TG and DTA curves of **I**.

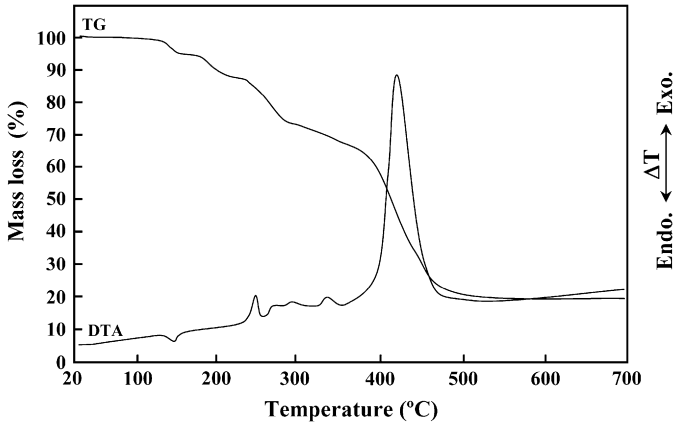

Fig. 13. TG and DTA curves of **III**.

the ν(C=N) stretching of *o*-vanillinato-1,2-ethylenediimin. All the complexes show a broad band of strong intensity in the range of 3642–3112 cm^{-1} assigned to the ν(O–H) of aqua ligand. The phenolic C–O stretching bands of the complexes of **I**, **II** and **III** are observed at 1334 cm^{-1}, 1330 cm^{-1} and 1328 cm^{-1}, respectively (Fig. 10). Similar C–O stretching bands are reported in a previous work of salicylidene-2-aminobenzimidazole complexes [28].

3.3. Thermal behaviour

Thermal decomposition of *trans*-[Cu(*o*-van)$_2$(H_2O)$_2$] **I** (Fig. 11) and *cis*-[Cu(*o*-van)$_2$$H_2O$] **II** (Fig. 12), takes place in a similar manner and proceeds in three stages. The thermal dehydration stage of **I** occurs in two steps in the temperature range of 70–134 °C, accompanied by the endothermic effects (DTA_{max}: 95 and 122 °C). The weight loss (exp. 8.69%, theor. 8.96%) corresponds to the loss of two coordinated water molecules. The thermal dehydration stage of **II** occurs in one step in the temperature range of 104–139 °C, accompanied by the endothermic effects (DTA_{max}: 122 °C). The weight loss (exp. 5.26%, theor. 4.69%) corresponds to the loss of one coordinated water molecule. The second stage for **I** and **II** are related to the decomposition of *o*-vanillinato ligands, in the temperature ranges of 219–248 °C (DTA_{max}: 242 °C) and 202–245 °C (DTA_{max}: 226 °C), respectively. The exothermic decomposition for *trans*-isomer (**I**) is observed to be more intense than *cis*-isomer (**II**). On the basis of the first DTA_{max} of the anhydrous complexes, the thermal stability sequence is *trans*-isomer > *cis*-isomer. This fact should be related with the binding of the ligand. The similar sequence is reported in a previous work of the complexes with the Schiff bases *cis*- and *trans*-*N*,*N*′-bis(salicylidene)-1,2-ciclohexadiamines [29]. In the third stage for **I** and **II**, strong exothermic peaks of DTA curves are associated with the burning of the organic residue. The final decomposition product, namely CuO, was identified by IR spectroscopy. The overall weight loss for **I** and **II** (exp. 76.71%, theor. 80.20 and exp. 78.69%, theor. 79.28%, respectively) agrees well with the given structure.

The decomposition of **III** takes place in four stages (Fig. 13). The first stage is related to the dehydration of the complex in the temperature range of 118–165 °C, accompanied by endothermic effect (DTA_{max}: 143 °C). The weight loss (exp. 4.80%, theor. 4.41%) corresponds to the loss of one coordinated water molecule. The second and third stages are related to the decomposition of the Schiff base. The fourth stage of the complex related to the strong exothermic DTA peak is associated with the burning of the organic residue. The final decomposition product, namely CuO, was identified by IR spectroscopy. The overall weight loss (exp. 80.77%, theor. 80.49%) for **III** agrees well with the given structure.

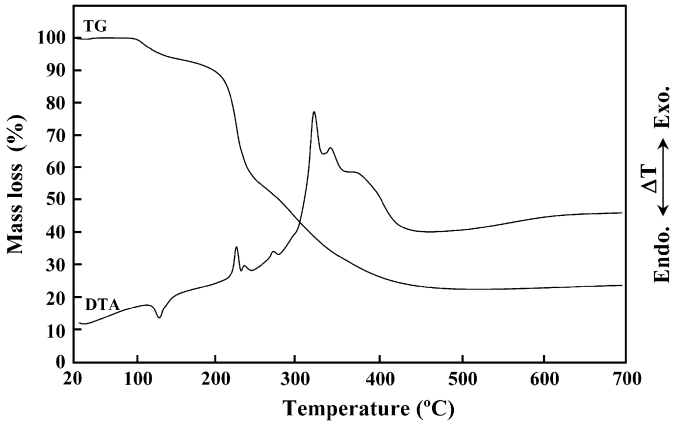

Fig. 12. TG and DTA curves of **II**.

References

[1] Enikolopyan NS, Bogdanova KA, Askarov KA. Russ Chem Rev 1983;52:13–25.
[2] Leung WH, Che CM. Inorg Chem 1989;28:4116–21.
[3] El-Hendawy AM, Alkubaisi AH, El-Ghany A, El-Korashy K, Sharab MN. Polyhedron 1993;12:2343–50.
[4] McCarthy PJ, Hovey RJ, Veno K, Martell AE. J Am Chem Soc 1955;77:5820–7.
[5] Barton JK. Science 1986;233:727–34.
[6] Burrows CJ, Muller JG. Chem Rev 1998;98:1109–52.
[7] Erkkila KE, Odom DT, Barton JK. Chem Rev 1999;99:2777–96.
[8] Delaney S, Pascaly M, Bhattacharya PK, Han K, Barton JK. Inorg Chem 2002;41:1966–74.
[9] Crowe AJ, Smith PJ, Atassi G. Chem Biol Interact 1980;32:171–8.

[10] Wang M, Wang LF, Li YZ, Li QX, Xu ZD, Qu DM. Transition Met Chem 2001;26:307–10.
[11] Dhumwad SD, Gudasi KB, Goudar TR. Indian J Chem 1994;33A:320–4.
[12] Reddy KH, Reddy PS, Babu PR. Transition Met Chem 2000;25:154–60.
[13] Singh H, Yadav LDS, Mishra SBS. J Inorg Nucl Chem 1981;43:1701–4.
[14] Singh NK, Singh SB. Indian J Chem 2001;40A:1070–5.
[15] Mishra V, Pandeya SN, Anathan S. Acta Pharm Turc 2000;42(4): 139–45.
[16] Jouad EM, Riou A, Allian M, Khan MA, Bouet GM. Polyhedron 2001;20:67–74.
[17] Chandra S, Gupta K. Transition Met Chem 2002;27:196–9.
[18] Dhiman AM, Wadodkar KN. Indian J Chem 2001;40B:636–9.
[19] Oleksyn B. Hung Diff Conf 1976;8:19. refcode MXSALC.
[20] Odabaşoğlu M, Albayrak Ç, Büyükgüngör O. Acta Crystallogr 2005; E61:o425–6.
[21] Stoe&Cie. X-AREA (version 1.18) and X-RED32 (version 1.04). Darmstadt, Germany: Stoe&Cie; 2002.
[22] Sheldrick GM. SHELXS97 and SHELXL97. Germany: University of Gottingen; 1997.
[23] Farrugia LJ. ORTEP3 for Windows. J Appl Crystallogr 1997;30:565.
[24] Farrugia LJ. WinGX – a Windows program for crystal structure analysis. Scotland: University of Glasgow; 1999.
[25] Kong D, Xie Y, Xie Y, Huang X. J Chem Crystallogr 1999;29:295–8.
[26] Khandar AA, Nejati K. Polyhedron 2000;19:607–13.
[27] Root CA, Hoeschele JD, Cornman CR, Kampt JW, Pecoraro VL. Inorg Chem 1993;32:3855–9.
[28] Mohammed GG, Abd El-Wahab ZH. J Therm Anal Calorim 2003;73:347–59.
[29] Cavalheiro ETG, Lemos FCD, Schpector JZ, Dockal ER. Thermochim Acta 2001;370:129–33.